JOURNAL OF CHEMICAL INFORMATION AND MODELING

Letter

pubs.acs.org/jcim

Kinetic Characterization of Fragment Binding in AmpC β-Lactamase by High-Throughput Molecular Simulations

P. Bisignano,[†,○] S. Doerr,[⊥,○] M. J. Harvey,[‡] A. D. Favia,[†,§] A. Cavalli,*[,†,∥] and G. De Fabritiis*[,⊥]

[†]Department of Drug Discovery and Development, Istituto Italiano di Tecnologia, via Morego, 30, 16163 Genova, Italy

[‡]Acellera, c/o PRBB, C/Dr Aiguader 88, 08003 Barcelona, Spain

[∥]Department of Pharmacy and Biotechnology, Università di Bologna, via Belmeloro 6, 40126 Bologna, Italy

[⊥]Computational Biophysics Laboratory, GRIB-IMIM, Universitat Pompeu Fabra, Dr. Aiguader 88, 08003 Barcelona, Spain

Supporting Information

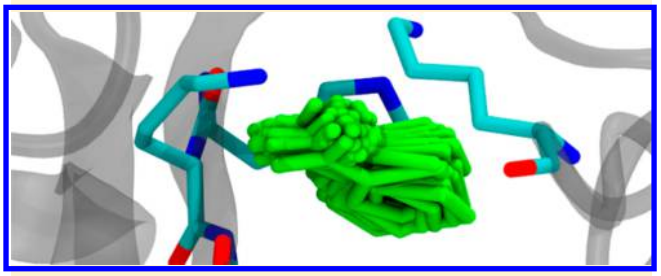

ABSTRACT: Small molecules used in fragment-based drug discovery form multiple, promiscuous binding complexes difficult to capture experimentally. Here, we identify such binding poses and their associated energetics and kinetics using molecular dynamics simulations on AmpC β-lactamase. Only one of the crystallographic binding poses was found to be thermodynamically favorable; however, the ligand shows several binding poses within the pocket. This study demonstrates free-binding molecular simulations in the context of fragment-to-lead development and its potential application in drug design.

INTRODUCTION

Fragment-based (FB) methods[1] have recently emerged as alternatives to traditional high throughput screenings (HTS) for the identification of starting hits in drug discovery programs.[2] The small size of the fragments (<300 Da) allows the exploration of a wider chemical space relative to larger lead-like compounds and has showed an enhanced probability of finding hits.[3−5] Fragments, however, usually have binding affinities for their target in the micromolar to millimolar range, thus requiring the use of highly sensitive and low-throughput biophysical techniques, including nuclear magnetic resonance (NMR),[6−8] surface plasmon resonance (SPR),[7,9] or isothermal titration calorimetry (ITC).[10,11] Such methods can be used in conjunction with X-ray crystallography[10,12,13] to gain detailed structural information useful for the subsequent fragment growth.

A primary challenge in drug design is the determination of "good" fragment−protein complexes, i.e. those both energetically favorable and kinetically stable (high residence time). X-ray experiments usually determine just the most favorable poses, regardless of residence times, while experimental measures of fragment kinetics are difficult to obtain because of the fast rates involved. Since drug binding kinetics (i.e., k_{on} and k_{off} of interaction) are directly related to the length of time a drug spends in contact with its target, they are considered to be at least as important as the binding affinity.[14,15] Notably, drug−target binding kinetics of new molecules is seldom investigated, and then only retrospectively, in postlaunch analyses. A tool able to provide insights into alternative binding would be of outstanding utility to drug designers.[14,16]

Unfortunately, established in silico screening methods such as docking have been shown to be less effective when ranking protein−fragment complexes.[17,18] Although some success stories have been reported,[19] this can be generally ascribed to the low affinity of fragments for their targets[20] that leads to several iso-equivalent poses. In this context, microsecond-long molecular dynamics (MD) simulation is emerging as a promising tool for the identification of protein−ligand binding complexes.[21−24] It has been reported that such simulations are also able to estimate drug binding kinetics.[21]

As a test case for this method we selected, from the SERAPhiC database,[25] *Escherichia coli* AmpC β-lactamase in complex with carboxy-thiophene (see Figure 1A).[13] This choice was based on two factors: (i) the crystal structure shows multiple binding poses and (ii) the enzyme plays a major role in antibiotic-resistance and, as such, has been extensively investigated.[26,27] We ran high-throughput MD simulations,[21,28−31] producing 148 μs of aggregate trajectory, from which we identified multiple binding poses with comparable residence time to the crystallographic poses. From these, one requires partial rearrangement of a loop. It is very valuable to be able to reveal these hidden sites as they highlight strong interaction networks between the fragment and the protein.

RESULTS

The crystal structure of *E. coli* AmpC β-lactamase in complex with carboxy-thiophene (PDB ID: 2HDQ, chain A), Figure 1A, has a very large binding pocket that spans the active site, called the oxyanion hole, in which S64 plays a catalytic role; the distal site and the tunnel site together expand into a back pocket. This tunnel site can be found in open or closed conformation, depending on the gating residue K290.[13] The back pocket is

Published: January 20, 2014

   dx.doi.org/10.1021/ci4006063 | *J. Chem. Inf. Model.* 2014, 54, 362−366

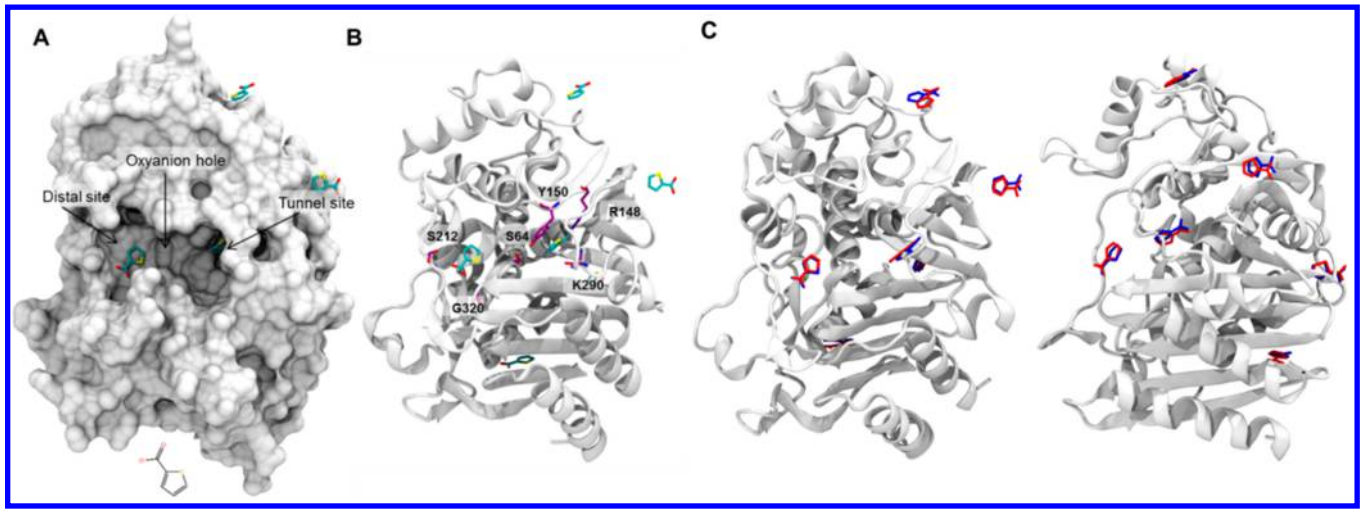

Figure 1. (A) Crystal structure of *E. coli* β-lactamase in complex with carboxy-thiophene. Ligand 2D structure is also reported at the bottom. (B) Protein fragment interactions. Representative residues in the binding site are also shown. (C) Poses matched between simulations and crystal structure. The red poses are crystal native, and the blue ones are the closest poses during ~148 μs of simulations.

Table 1. Binding Affinity and Kinetics Are Reported for All the Clusters[a]

cluster	K_{off} (s^{-1})	residence time (ns)	K_{on} (M^{-1} s^{-1})	binding time (ns)	K_D (M)	ΔG_{calc} (kcal/mol)
A	$1.95 \pm 0.07 \times 10^{6}$	$5.13 \pm 0.19 \times 10^{2}$	$2.18 \pm 0.07 \times 10^{9}$	$1.15 \pm 0.04 \times 10^{2}$	$8.96 \pm 0.41 \times 10^{-4}$	**-4.26 ± 0.02**
B	$1.67 \pm 0.06 \times 10^{6}$	$5.98 \pm 0.23 \times 10^{2}$	$2.90 \pm 0.14 \times 10^{8}$	$8.64 \pm 0.42 \times 10^{2}$	$5.79 \pm 0.43 \times 10^{-3}$	-2.96 ± 0.08
C	$1.63 \pm 0.06 \times 10^{6}$	**$6.16 \pm 0.22 \times 10^{2}$**	$6.87 \pm 0.69 \times 10^{7}$	$3.67 \pm 0.39 \times 10^{3}$	$2.39 \pm 0.27 \times 10^{-2}$	-2.36 ± 0.09
D	$2.43 \pm 0.12 \times 10^{6}$	$4.12 \pm 0.20 \times 10^{2}$	$8.92 \pm 0.63 \times 10^{7}$	$2.82 \pm 0.21 \times 10^{3}$	$2.74 \pm 0.26 \times 10^{-2}$	-1.92 ± 0.06
E	$1.11 \pm 0.10 \times 10^{7}$	90.67 ± 8.52	$2.13 \pm 0.16 \times 10^{7}$	$1.09 \pm 0.07 \times 10^{4}$	0.48 ± 0.06	-1.11 ± 0.07

[a]Cluster A shows the lowest free energy, while cluster C has the highest residence time. Residence time is calculated as the mean first passage time from the cluster to the bulk cluster, while binding time is calculated as the mean first passage time from the bulk cluster to the specific cluster. Error estimates were calculated by performing 100 bootstrapping iterations, in which 20% of the total simulations were randomly eliminated.

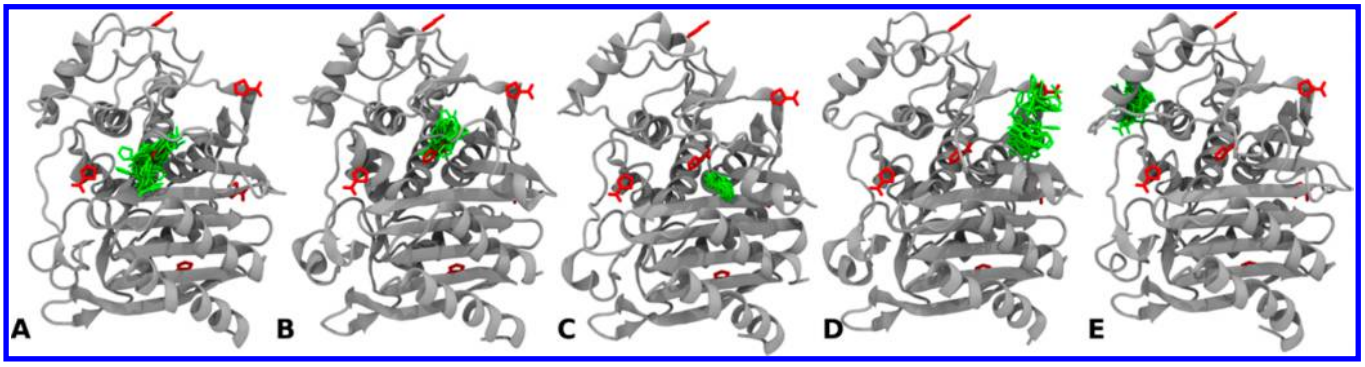

Figure 2. Protein in gray cartoon is taken from the crystal 2HDQ chain A, with the ligand's crystal poses shown in red. Clusters A, B, C, D, and E are shown in green. Cluster A which covers the oxyanion hole and the crystal pose has the lowest free energy, while clusters B and C have equivalent residence time to cluster A.

only fully evident in the presence of the ligand; it is formed by the partial unwinding of an α-helix and the insertion of K290 back into the protein where it interacts with both the protein and the ligand. This is plainly evident once apo (3BLS) and holo (2HDQ) structures are compared: the conformation of residues 279 to 293, shifts from a full helix with K290 pointing outward to a more coiled loop with K290 pointing inward (Supporting Information Figure S1). Key residues are shown in Figure 1B. In the crystal complex, the carboxy−thiophene does not lie in the oxyanion hole (S64). The most representative binding pose is near the core of the active site of the enzyme, making $\pi-\pi$ interactions with Y150 and a salt bridge with R148. When in the distal site, the fragment makes two hydrogen bonds with the backbone amides of S212 and G320.[13]

All but the two poses in the binding pocket region seemed stabilized by the crystal packing or saturation effects (See Supporting Information Figure S2). Moreover if we superpose the two chains (Supporting Information Figure S3), we can notice that, in the binding site, only the pose in the distal site is reproduced in both monomers. However, looking at the simulations that reach the distal site and the tunnel site crystal poses, we see that even though both are reached within tens of nanoseconds, only the pose in the tunnel site is stable while the distal site pose is only visited transiently in 13 simulations (Supporting Information Figure S4).

dx.doi.org/10.1021/ci4006063 | J. Chem. Inf. Model. 2014, 54, 362−366

Free Ligand Binding. Ligand binding simulations of carboxy-tiophene diffusing around the AmpC β-lactamase were performed on GPUGRID,[29] resulting in 148 μs of aggregate simulation time. During the simulations the ligand was allowed to diffuse freely through the solvent into the protein without any biasing potentials.

A first analysis of the results showed that all six binding poses were visited by MD (Figure 1C), but with very different thermodynamic features as most of these were not particularly stable.

Simulation Multiple Binding Mode Analysis. The trajectories were analyzed using a Markov state model analysis method, derived from ref 21 which allows the complete reconstruction of the binding process in terms of kinetics (k_{on}, k_{off}) and affinities (ΔG^0) for each pose (see Methods). The various bound complexes generated via MD simulations were grouped into six kinetically distinct clusters, one of which represented the bulk. For each pose k_{off}, residence time ($1/k_{off}$), k_{on}, mean first passage time for binding from the bulk, $k_D = k_{off}/k_{on}$ and ΔG were calculated (Table 1). For details on the calculation of ΔG see the Supporting Information.

The pose in the oxyanion hole (cluster A Figure 2, which covers most of the binding site) was found to be most stable, as judged by ΔG (Table 1, data of cluster A). As shown in Figure 2, the rest of the clusters span the tunnel site (clusters B and C) as well as the side and back of the protein (clusters D and E). Cluster C is the most spatially compact, being more kinetically separated from the rest, while the remainder cover broader regions due to fast interconversions within them.

Resident and Energetically Favorable Poses. Cluster A (Figure 2A) with standard binding affinity of -4.26 kcal mol^{-1} is the most thermodynamically favored. The high affinity of cluster A is unsurprising as it overlaps the crystallographic binding pose of the carboxy-thiophene in the tunnel site as well as the oxyanion hole. Visual inspection of a typical binding pathway (see ci4006063_si_001.avi in the Supporting Information) shows how the negatively charged carboxy-thiophene can span the whole positively charged AMPC β-lactamase binding site. It is unsurprising therefore that cluster A spans most of the pocket as the poses within it interchange very rapidly as the entire pocket forms a deep energetic well from which the ligand cannot easily escape. Due to the establishment of weak interactions within the distal site and the oxyanion hole, the fragment does not achieve thermodynamically stable binding modes, while in the tunnel site interactions are stronger.

Accordingly, cluster C (Figure 2C), which is located in the tunnel site has a residence time of 616 $\pm$ 22 ns, similar to the 513 $\pm$ 19 ns of cluster A. Surprisingly, we found that it did not superimpose onto any of the crystallographic poses. In fact, it corresponded to a binding mode in which the ligand was deeply buried into the tunnel site, and this pose was comparably stable to the most resident of the crystallographic poses. The reason why it is not as thermodynamically favorable as cluster A is due to its low k_{on} which is caused by the loop in residues 279 to 293 having to open for carboxy-thiophene to enter.

For carboxy-thiophene to reach cluster C it first has to pass from cluster A (oxyanion hole and tunnel site) before entering (see ci4006063_si_002.avi in the Supporting Information). As cluster A is an intermediate for the entering and exiting of the ligand into cluster C, cluster C has a higher residence time than A. The loop can then close and further stabilize the ligand, requiring around 100 ns for the loop to open again and the ligand to move from C to A.

Loop Interactions in the Tunnel Site. It is interesting to note that in the simulations the tunnel site and back pocket are formed by the partial unwinding of an α-helix, corresponding to that seen in the crystal structure.

The loop is able to visit both the open and closed conformations in the absence of the ligand. However, when the ligand interacts with the loop it is able to stabilize its open conformation while entering the tunnel site and stabilize its closed conformation when inside.

Once inside the tunnel site, the ligand can insert deeply into the tunnel site (cluster C) and interacts with additional residues, which stabilize it further. In the deeply inserted state, the ligand's carboxylic moiety interacts electrostatically with the amino group of K315 and also with K290, whose inward conformation is stabilized by a loop-closing salt bridge with E272 (see Figure 3 for the interaction network). Additionally

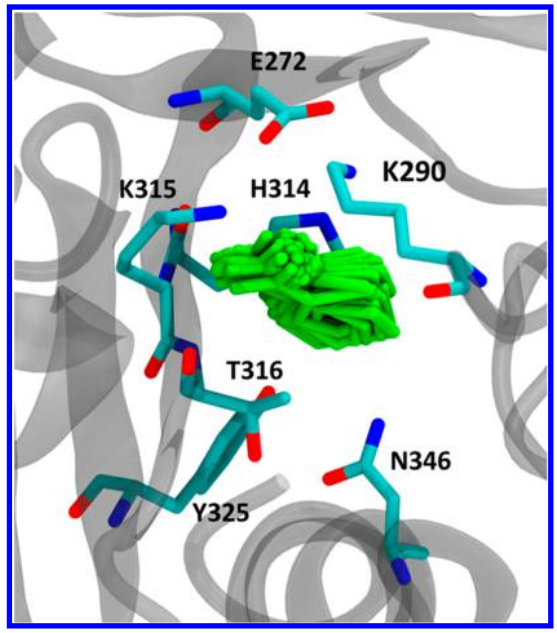

Figure 3. Interaction network. This picture shows the residues of the protein within 3 Å of the ligand for cluster A. Salt bridges within the protein: E272−K290 and T316−N346 contribute to hiding the back pocket in which the ligand is buried, giving high residence time. The ligand interacts with K290, stretching the conformation of the secondary structure the residue belongs to, so the lysine is pointing inward. While most of the residues in the binding pocket are quite stable during dynamics, K290 is mobile. Accordingly, the flexible loop that can be seen as the gate-keeper of the tunnel site.

the fragment creates a hydrogen bond with the hydroxyl of T316 and the amino group of N346, which even can form a salt bridge within the protein, interacting with Y325 contributing to the hiding of the back pocket.

DISCUSSION AND CONCLUSIONS

In this study, MD simulations were able to recover all six crystallographic poses that a small fragment is known experimentally to adopt in the AmpC β-lactamase binding site. In addition, our MD analysis showed that these poses were kinetically and thermodynamically distinct with some displaying higher stability than others. Our study also identified previously

dx.doi.org/10.1021/ci4006063 | J. Chem. Inf. Model. 2014, 54, 362−366

undisclosed binding poses, with comparable residence time to a crystallographic pose.

In one of these equally stable poses the ligand binds deeper in the tunnel site by making stronger interactions with K290, the gatekeeper of the tunnel site.

In particular, residence time—which is related to the protein−ligand unbinding k_{off}—is a significant parameter to optimize in order to improve drug efficacy in vivo.[14,16] Although the association rate can vary widely among receptor−ligand pairs,[32] it is fundamentally limited by the diffusion between the two species in physiological solutions (10^8−10^9 M^{-1} s^{-1}); whereas, residence time depends on the interaction network between the two molecular species.[14] Moreover, the likelihood of a ligand−receptor association is related to the local ligand concentration due to its ADME (adsorption, distribution, metabolism, and excretion) profile. In contrast, the receptor−ligand dissociation rate is independent of those factors, being rather a function of the specific interactions between the two species (such as conformational rearrangements, polar forces, hydrogen bonds, and van der Waals interactions).[14,33]

The ability to accurately predict binding kinetics would be of outstanding utility in drug design, especially for the hit-to-lead and lead optimization phases.[14,16] However, experimental assessments of fragment kinetics are challenging because of promiscuous binding and fast time scales involved.

Our study demonstrates that computational simulations using molecular dynamics can play an important role in drug discovery, mainly thanks to the possibility to identify novel binding modes and to assess at an early stage the binding kinetics. Describing binding kinetics allows one to draw a more detailed free energy landscape and could possibly point the synthetic chemistry efforts toward exploiting those minima that are due to high quality interactions. These interactions facilitate the process of converting a fragment into a lead-like compound with optimized kinetics and affinity profiles.

METHODS

System Preparation. The input model was based on the crystallographic structure of the fragment inhibitor carboxythiophene bound to *E. coli* β-lactamase (PDB: 2HDQ chain A). The protein was modeled with the AMBER99SB force field[34] and the ligand with the GAFF force field.[35] Fifty systems were built, starting from 50 different arbitrary ligand positions, at least 15 Å away from the protein. Models were ionized and solvated with TIP3P water molecules, setting unit cell dimensions to 80 Å × 80 Å × 80 Å. Resultant systems contained between 47 000 and 48 000 atoms. These systems were minimized and equilibrated locally with ACEMD[31] for 2 ns under *NPT* conditions, of 1 atm at 300 K, nonbonded cutoff of 9 Å, rigid bonds, and PME electrostatics. A time step of 4 fs was used, in conjunction with a hydrogen mass repartitioning scheme.[36]

During minimization and the first 1 ns of equilibration, the protein's Cα and ligand's heavy atoms were restrained by a harmonic potential with k = 1 kcal mol^{-1} $Å^{-2}$. During the equilibration the ligand was kept at least 10 Å from the center of mass of the protein by applying a harmonic repulsive potential between protein and ligand with k = 5 kcal mol^{-1} $Å^{-2}$.

After equilibration, pressure control was disabled and thirty replicas were built for each equilibrated system. The resulting 1500 simulations were run on GPUGRID.[29] During production, no biasing potentials were imposed: the ligand was allowed to diffuse freely through the solvent into the protein. Data retrieval resulted in 1496 distinct trajectories of lengths between 50 and 150 ns. Due to the relatively low k_{on} of cluster C, to better sample the binding event and loop dynamics of the cluster, we respawned 75 more simulations of 100 ns from cluster C with the loop open and 25 more with the loop closed which improved the estimates of the kinetics. This provided a total of 1 482 076 configurations of free carboxytiophene diffusing around the AmpC β-lactamase, about 148 μs of total aggregate trajectory.

MD Simulation Analysis. Markov state models (MSM) are a useful tool for statistically describing the dynamics of a system using the probabilities of transitions between coarse-grained states.[37] From the Markov model we obtained a dynamic description of the binding process. Conformations were defined according to a binary ligand−protein contact map, described by the contacts between ligand atoms C1 and C6 and all the CA atoms of the protein, using a threshold of 8 Å.

Conformations were first clustered using the k-centers algorithm according to their contact map similarities and then their time dynamics modeled using a Markov model. From the 100 clusters produced, 21 were poorly populated and thus were merged into their closest neighbor, resulting in 79 clusters. Convergence of the Markov model was determined by analysis of the implied time scales (Supporting Information Figure S5) showing the time scales of the important dynamical processes present in the system. From the flattening-out of the two longest time scales, we conclude that models produced with a lag time >20 ns are Markovian and thus provide a good model of the processes present in the simulations.

The 79 clusters produced by k-centers were further grouped into six macrostates based on their kinetic similarity using Perron-cluster cluster analysis (PCCA).[38] Affinities and kinetics of binding were derived from a model constructed using a lag time of 20 ns. Error estimates of the affinities and kinetics were calculated by 100 bootstrapping iterations, in each of which 20% of the trajectories were randomly eliminated.

ASSOCIATED CONTENT

Supporting Information

Binding free energy calculation details. Five figures: S1 a comparison of apo and holo structures; S2 chains A and B of PDB 2HDQ; S3 ligand poses of aligned chains A and B of 2HDQ; S4 binding events of two crystal poses in the pocket; S5 Markov model implied time scales. Two video files as described in the text. This material is available free of charge via the Internet at http://pubs.acs.org.

AUTHOR INFORMATION

Corresponding Authors

*A.C. E-mail: Andrea.Cavalli@iit.it.

*G.D.F. E-mail: gianni.defabritiis@upf.edu.

Present Address

§(A.D.F.) Lilly China R&D Centre (LCRDC), Eli Lilly and Company, Building 8, No 338, Jia Li Lue Road, Shanghai 201203, China.

Author Contributions

○P.B. and S.D. contributed equally.

Notes

The authors declare no competing financial interest.

■ ACKNOWLEDGMENTS

G.D.F. acknowledges support by the Spanish Ministry of Science and Innovation (BIO2011-27450). We thank all volunteers of GPUGRID who donated GPU computing time to the project.

■ ABBREVIATIONS

FB, fragment-based; HTS, high throughput screening; NMR, nuclear magnetic resonance; SPR, surface plasmon resonance; ITC, isothermal titration calorimetry; PDB, protein data bank; MSM, Markov state modeling

■ REFERENCES

(1) Warr, W. A. Fragment-Based Drug Discovery. *J. Comput. Aided Mol. Des.* **2009**, *23*, 453−458.
(2) Whittaker, M.; Law, R. J.; Ichihara, O.; Hesterkamp, T.; Hallett, D. Fragments: Past, Present and Future. *Drug Discov. Today Technol.* **2010**, *7*, e163−e171.
(3) Congreve, M.; Chessari, G.; Tisi, D.; Woodhead, A. J. Recent Developments in Fragment-Based Drug Discovery. *J. Med. Chem.* **2008**, *51*, 3661−3680.
(4) Hajduk, P. J.; Greer, J. A Decade of Fragment-Based Drug Design: Strategic Advances and Lessons Learned. *Nat. Rev. Drug Discov.* **2007**, *6*, 211−219.
(5) Hann, M. M.; Leach, A. R.; Harper, G. Molecular Complexity and Its Impact on the Probability of Finding Leads for Drug Discovery. *J. Chem. Inf. Comput. Sci.* **2001**, *41*, 856−864.
(6) Jacobsen, J. A.; Fullagar, J. L.; Miller, M. T.; Cohen, S. M. Identifying Chelators for Metalloprotein Inhibitors Using a Fragment-Based Approach. *J. Med. Chem.* **2011**, *54*, 591−602.
(7) Ward, R. A.; Brassington, C.; Breeze, A. L.; Caputo, A.; Critchlow, S.; Davies, G.; Goodwin, L.; Hassall, G.; Greenwood, R.; Holdgate, G. A.; Mrosek, M.; Norman, R. A.; Pearson, S.; Tart, J.; Tucker, J. A.; Vogtherr, M.; Whittaker, D.; Wingfield, J.; Winter, J.; Hudson, K. Design and Synthesis of Novel Lactate Dehydrogenase A Inhibitors by Fragment-Based Lead Generation. *J. Med. Chem.* **2012**, *55*, 3285−3306.
(8) Barelier, S.; Pons, J.; Marcillat, O.; Lancelin, J.-M.; Krimm, I. Fragment-Based Deconstruction of Bcl-xL Inhibitors. *J. Med. Chem.* **2010**, *53*, 2577−2588.
(9) Geitmann, M.; Elinder, M.; Seeger, C.; Brandt, P.; de Esch, I. J. P.; Danielson, U. H. Identification of a Novel Scaffold for Allosteric Inhibition of Wild Type and Drug Resistant HIV-1 Reverse Transcriptase by Fragment Library Screening. *J. Med. Chem.* **2011**, *54*, 699−708.
(10) Gozalbes, R.; Carbajo, R. J.; Pineda-Lucena, A. Contributions of Computational Chemistry and Biophysical Techniques to Fragment-Based Drug Discovery. *Curr. Med. Chem.* **2010**, *17*, 1769−1794.
(11) Edink, E.; Jansen, C.; Leurs, R.; de Esch, I. J. P. The Heat Is on: Thermodynamic Analysis in Fragment-Based Drug Discovery. *Drug Discov. Today Technol.* **2010**, *7*, e189−e201.
(12) Murray, C. W.; Carr, M. G.; Callaghan, O.; Chessari, G.; Congreve, M.; Cowan, S.; Coyle, J. E.; Downham, R.; Figueroa, E.; Frederickson, M.; Graham, B.; McMenamin, R.; O'Brien, M. A.; Patel, S.; Phillips, T. R.; Williams, G.; Woodhead, A. J.; Woolford, A. J.-A. Fragment-Based Drug Discovery Applied to Hsp90. Discovery of Two Lead Series with High Ligand Efficiency. *J. Med. Chem.* **2010**, *53*, 5942−5955.
(13) Babaoglu, K.; Shoichet, B. K. Deconstructing Fragment-Based Inhibitor Discovery. *Nat. Chem. Biol.* **2006**, *2*, 720−723.
(14) Copeland, R. A.; Pompliano, D. L.; Meek, T. D. Drug−target Residence Time and Its Implications for Lead Optimization. *Nat. Rev. Drug Discov.* **2006**, *5*, 730−739.
(15) Swinney, D. C. Biochemical Mechanisms of Drug Action: What Does It Take for Success? *Nat. Rev. Drug Discov.* **2004**, *3*, 801−808.
(16) Ladbury, J. E.; Klebe, G.; Freire, E. Adding Calorimetric Data to Decision Making in Lead Discovery: A Hot Tip. *Nat. Rev. Drug Discov.* **2010**, *9*, 23−27.
(17) Murray, C. W.; Verdonk, M. L.; Rees, D. C. Experiences in Fragment-Based Drug Discovery. *Trends Pharmacol. Sci.* **2012**, *33*, 224−232.
(18) Bottegoni, G.; Favia, A. D.; Recanatini, M.; Cavalli, A. The Role of Fragment-Based and Computational Methods in Polypharmacology. *Drug Discov. Today* **2012**, *17*, 23−34.
(19) Chen, Y.; Shoichet, B. K. Molecular Docking and Ligand Specificity in Fragment-Based Inhibitor Discovery. *Nat. Chem. Biol.* **2009**, *5*, 358−364.
(20) Bisignano, P.; Lambruschini, C.; Bicego, M.; Murino, V.; Favia, A. D.; Cavalli, A. In Silico Deconstruction of ATP-Competitive Inhibitors of Glycogen Synthase Kinase-3β. *J. Chem. Inf. Model.* **2012**, *52*, 3233−3244.
(21) Buch, I.; Giorgino, T.; De Fabritiis, G. Complete Reconstruction of an Enzyme-Inhibitor Binding Process by Molecular Dynamics Simulations. *Proc. Natl. Acad. Sci. U.S.A.* **2011**, *108*, 10184−10189.
(22) Silva, D.-A.; Bowman, G. R.; Sosa-Peinado, A.; Huang, X. A Role for Both Conformational Selection and Induced Fit in Ligand Binding by the LAO Protein. *PLoS Comput. Biol.* **2011**, *7*, e1002054.
(23) Held, M.; Metzner, P.; Prinz, J.-H.; Noé, F. Mechanisms of Protein-Ligand Association and Its Modulation by Protein Mutations. *Biophys. J.* **2011**, *100*, 701−710.
(24) Shan, Y.; Kim, E. T.; Eastwood, M. P.; Dror, R. O.; Seeliger, M. A.; Shaw, D. E. How Does a Drug Molecule Find Its Target Binding Site? *J. Am. Chem. Soc.* **2011**, *133*, 9181−9183.
(25) Favia, A. D.; Bottegoni, G.; Nobeli, I.; Bisignano, P.; Cavalli, A. SERAPhiC: A Benchmark for in Silico Fragment-Based Drug Design. *J. Chem. Inf. Model.* **2011**, *51*, 2882−2896.
(26) Drawz, S. M.; Bonomo, R. A. Three Decades of Beta-Lactamase Inhibitors. *Clin. Microbiol. Rev.* **2010**, *23*, 160−201.
(27) Bowman, G. R.; Geissler, P. L. Equilibrium Fluctuations of a Single Folded Protein Reveal a Multitude of Potential Cryptic Allosteric Sites. *Proc. Natl. Acad. Sci. U.S.A.* **2012**, *109*, 11681−11686.
(28) Sadiq, S. K.; Noé, F.; De Fabritiis, G. Kinetic Characterization of the Critical Step in HIV-1 Protease Maturation. *Proc. Natl. Acad. Sci. U.S.A.* **2012**, *109*, 20449−20454.
(29) Buch, I.; Harvey, M. J.; Giorgino, T.; Anderson, D. P.; De Fabritiis, G. High-Throughput All-Atom Molecular Dynamics Simulations Using Distributed Computing. *J. Chem. Inf. Model.* **2010**, *50*, 397−403.
(30) Giupponi, G.; Harvey, M. J.; De Fabritiis, G. The Impact of Accelerator Processors for High-Throughput Molecular Modeling and Simulation. *Drug Discov. Today* **2008**, *13*, 1052−1058.
(31) Harvey, M. J.; Giupponi, G.; Fabritiis, G. D. ACEMD: Accelerating Biomolecular Dynamics in the Microsecond Time Scale. *J. Chem. Theory Comput.* **2009**, *5*, 1632−1639.
(32) Fersht, A. *Structure and Mechanism in Protein Science: A Guide to Enzyme Catalysis and Protein Folding*; W.H. Freeman: New York, 1999.
(33) Lu, H.; Tonge, P. J. Drug-Target Residence Time: Critical Information for Lead Optimization. *Curr. Opin. Chem. Biol.* **2010**, *14*, 467−474.
(34) Hornak, V.; Abel, R.; Okur, A.; Strockbine, B.; Roitberg, A.; Simmerling, C. Comparison of Multiple Amber Force Fields and Development of Improved Protein Backbone Parameters. *Proteins* **2006**, *65*, 712−725.
(35) Wang, J.; Wolf, R. M.; Caldwell, J. W.; Kollman, P. A.; Case, D. A. Development and Testing of a General Amber Force Field. *J. Comput. Chem.* **2004**, *25*, 1157−1174.
(36) Feenstra, K. A.; Hess, B.; Berendsen, H. J. C. Improving Efficiency of Large Time-Scale Molecular Dynamics Simulations of Hydrogen-Rich Systems. *J. Comput. Chem.* **1999**, *20*, 786−798.
(37) Noé, F.; Fischer, S. Transition Networks for Modeling the Kinetics of Conformational Change in Macromolecules. *Curr. Opin. Struct. Biol.* **2008**, *18*, 154−162.
(38) Deuflhard, P.; Weber, M. Robust Perron Cluster Analysis in Conformation Dynamics. *Linear Algebra Its Appl.* **2005**, *398*, 161−184.